

# International Journal of Applied Mathematics in Control Engineering

Journal homepage: <http://www.ijamce.com>

## Kalman Federal Filtering Algorithm of UAV Fault-Tolerant Integrated Navigation

Hongmei Zhang<sup>a,\*</sup>, Huaqing Zhang<sup>a</sup><sup>a</sup> College of Automation, Shenyang Aerospace University, Shenyang 110136, China

---

### ARTICLE INFO

## Article history:

Received 24 June 2008

Accepted 11 September 2008

Available online 28 October 2008

## Keywords:

Solar vector measuring device

CNS/SINS/GPS

Kalman federal filter

Fault-tolerant integrated navigation

---

### ABSTRACT

In this paper, a solar ray vector measuring device is designed which is used as a measurement sensor for the sub-filters of the federal filter, together with the magnetometer and accelerometer, then combine them with Global Positioning System (GPS) and Strap-down Inertial Navigation System (SINS) to form a federal filter fault-tolerant integrated navigation system. By making the attitude measured by the accelerometer and magnetic in the sub-filter as the initial value of the attitude in the navigation status, the navigation system can accurately estimate the value of attitude of any parking posture when the drone takes off. After the navigation system is started, the accelerometer and the magnetometer are used as the sub-filter's sensors of attitude measurement to form the Kalman federal filter integrated navigation system. The simulation results show that the Kalman federal filter designed in this paper can give the navigation status information with high accuracy, and when the magnetometer is disturbed or failing, the filter can still give the optimal estimation of the attitude as long as the current solar vector measuring device works normally, that improves the fault tolerance performance of the attitude information.

Published by Y.X.Union. All rights reserved.

## 1. Introduction

To improve the accuracy and stability of navigation system in aircraft or spacecraft and reduce the cost of sensors used in navigation system is the basic problems to be considered in the progress of designing navigation filtering algorithm. The papers [1],[2] have designed a Unscented Kalman filters based on Celestial Navigation System (CNS), SINS and GNSS(Global Navigation Satellite System), which have greatly improved accuracy of Navigation. A federal unscented Kalman filter for spacecraft navigation system based on SINS and CNS was proposed in [3], and adopting the method of multi-star vector observation to determine the attitude of spacecraft. Among them, the sensors of sensing star in system CNS have the characteristics of anti-electromagnetic interference, which can correct the output of attitude in inertial navigation system under the circumstance of strong electromagnetic interference. However, the navigation systems designed in literature [1]-[3] do not have sensor fault tolerance for attitude estimation. The filters will not be able to accurately estimate the attitude when the star sensors fail. In the paper [4], SINS, GNSS and visual positioning system were used to design the integrated navigation system of UAV, and the method of weighted least square was applied to select GNSS or visual positioning system and SINS for combination. So the visual

\* Corresponding author.

E-mail addresses: [zhang.hongmei@163.com](mailto:zhang.hongmei@163.com) (H. Zhang)

positioning system could still be used to assist the UAV to positioning when the signal of GNSS is weak. The schemes in papers [5] and [6] have improved Kalman filtering algorithms, then the errors of attitude in the navigation system have a fast convergence speed and a high accuracy when the UAV is disturbed. The paper [7] developed a new filter based on the extended Kalman filtering algorithms and the separated differential Kalman filtering algorithms where the predictive error covariance matrix was adjusted by using the fault adjustment factor, and the simulation results have verified that the algorithms have fault tolerance for system faults and measured faults to some extent. In paper [8], an adaptive Kalman filtering algorithm which has the ability of interference suppression ability, was proposed to perform initial estimation and real-time update of UAV attitude quaternions. In reference [9], the SINS/GNSS/CNS combined navigation federated filtering algorithm was proposed, which integrated the long time high accurate positioning of GNSS and the more accurate attitude measurement auxiliary SINS of CNS. The simulation results show that the algorithm has high convergence speed and accuracy.

Although CNS has higher precision, it is greatly affected by the light. The geomagnetic vector measured by the magnetometer is more accurate, but it is extremely susceptible to electromagnetic interference. Based on the advantages and disadvantages of CNS and magnetometer, a solar vector measurement device is designed.

It is combined with magnetometer and accelerometer as the measuring sensor of the federal filter neutron filter and GPS and SINS as the federal filter fault-tolerant integrated navigation system. Simulation results show that not only the integrated navigation system can only output very accurate navigation information, but also the attitude estimation of the filter will not be affected by the failure of the magnetometer.

## 2. The establishment of mathematical model of sensor

### 2.1 Design and modeling of solar vector measurement device

Build a four-sided platform on the upper surface of the drone fuselage. Five light panels with the same area are laid on the five surfaces of the regular four-sided platform, as shown in figure 1.

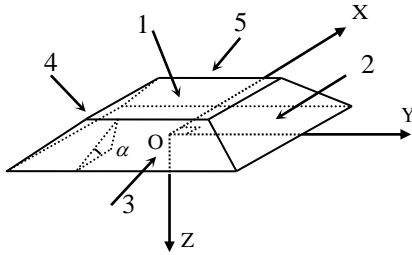


Fig.1. Solar vector measuring device

The light panels are labeled 1-5 respectively, which is the included Angle between the side light panels and the bottom plane, and the size is designed as. Then the unit normal vector of top light panel 1 and side light panel 2-5 in the machine system OXYZ is respectively expressed as

$$\begin{cases} \mathbf{n}_1 = [0 \ 0 \ -1]^T \\ \mathbf{n}_2 = \text{rot}_2(X, \alpha)[0 \ 0 \ -1]^T \\ \mathbf{n}_3 = \text{rot}_3(Y, -\alpha)[0 \ 0 \ -1]^T \\ \mathbf{n}_4 = \text{rot}_4(X, -\alpha)[0 \ 0 \ -1]^T \\ \mathbf{n}_5 = \text{rot}_5(Y, \alpha)[0 \ 0 \ -1]^T \end{cases} \quad (1)$$

where  $\text{rot}_j(X, \alpha)$  indicate rotation matrix when the normal vector is represented in machine system of light panels  $j(j \in [2, 3, 4, 5])$ .

The sun vector  $s$ , its deflection angle  $\zeta$  and roll angle  $\xi$  in the machine system are defined in the body coordinate system, as shown in figure 2. Sun vector under the machine system

$$\mathbf{s} = \begin{bmatrix} s_x \\ s_y \\ s_z \end{bmatrix} = \begin{bmatrix} \sin \zeta \\ \sin \xi \cos \zeta \\ \cos \xi \cos \zeta \end{bmatrix} \|\mathbf{s}\| \quad (2)$$

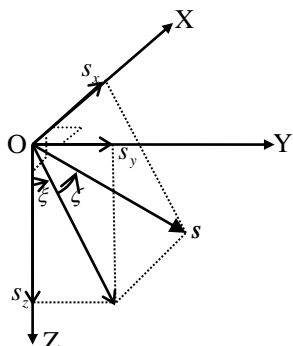


Fig.2. Representation of the solar vector in the body coordinate system

The direction cosine of the angle  $\theta_j$  between the unit normal vector of the  $j$  th photocell in the machine system and  $s$  is

$$\cos \theta_j = \frac{\mathbf{s} \mathbf{n}_j}{\|\mathbf{s}\|} \quad (3)$$

According to the photovoltaic effect and equation (3), the current generated by the  $j$  th photocell can be written as

$$I_j = I_{max} \cos \theta_j = I_{max} \frac{\mathbf{s} \mathbf{n}_j}{\|\mathbf{s}\|} \quad (4)$$

where,  $I_{max}$  is the maximum photocurrent when sunlight enters the solar panel vertically. Combining equations (1), (2) and (4), it can be concluded that the current measured by the no. 1 optical panel at the top is

$$I_1 = \frac{I_{max}}{\|\mathbf{s}\|} \mathbf{s} \mathbf{n}_1 = -I_{max} \cos \xi \cos \zeta \quad (5)$$

Similarly, the current measured by no. 2-5 solar panel is

$$I_j = \frac{I_{max}}{\|\mathbf{s}\|} \mathbf{s} \mathbf{n}_j = I_{max} \begin{bmatrix} \sin \zeta \\ \sin \xi \cos \zeta \\ \cos \xi \cos \zeta \end{bmatrix} (\text{rot}_j \begin{bmatrix} 0 \\ 0 \\ -1 \end{bmatrix}) \quad (6)$$

Parameters  $\zeta$ ,  $\xi$  and  $I_{max}$  can be obtained by the current expressions of the three optical panels with the maximum photocurrent. The unit sun vector can be solved in real time

$$\mathbf{s}_b^m = \begin{bmatrix} \sin \zeta \\ \sin \xi \cos \zeta \\ \sin \xi \cos \zeta \end{bmatrix} + \mathbf{n}_s \quad (7)$$

where  $\mathbf{n}_s$  is Gauss white noise vector with variance  $\sigma_s^2$ .

### 2.2 The establishment of inertial devices, magnetometer and GPS model

The mathematical model of angular velocity measured by gyroscope is

$$\boldsymbol{\omega}_b = \boldsymbol{\omega}_{true} + \mathbf{b}_w + \mathbf{n}_w \quad (8)$$

where,  $\boldsymbol{\omega}_b$  is the output vector of gyroscope,  $\mathbf{b}_w$  is the zero offset error vector of angular velocity, and  $\mathbf{n}_w$  is the random drift error vector of angular velocity.  $\mathbf{n}_w$  is the variance  $\sigma_w^2$  of Gauss white noise.

The mathematical model of the measured values of accelerometer and magnetometer is

$$\begin{cases} \mathbf{a}_b = \mathbf{a}_b^{true} + \mathbf{b}_a + \mathbf{n}_a \\ \mathbf{m}_b = \mathbf{m}_b^{true} + \mathbf{b}_m + \mathbf{n}_m \end{cases} \quad (9)$$

where  $(\mathbf{a}_b, \mathbf{m}_b)$ ,  $(\mathbf{b}_a, \mathbf{b}_m)$  and  $(\mathbf{n}_a, \mathbf{n}_m)$  are respectively the output vector, offset error vector and random drift error vector of accelerometer and magnetometer in the machine system.  $\mathbf{n}_a, \mathbf{n}_m$  are Gauss white noise with variance of  $\sigma_a^2$  and  $\sigma_m^2$  respectively.

The approximate measurement mathematical model of the GPS sensor is

$$\begin{cases} p_x^G = p_{xtrue}^G + n_g \\ p_y^G = p_{ytrue}^G + n_g \\ p_z^G = p_{ztrue}^G + n_{g_z} \\ v_x^G = v_{xtrue}^G + n_{g_v} \\ v_y^G = v_{ytrue}^G + n_{g_v} \\ v_z^G = v_{ztrue}^G + n_{g_{v_z}} \end{cases} \quad (10)$$

where  $p_{xtrue}^G, p_{ytrue}^G, p_{ztrue}^G, v_{xtrue}^G, v_{ytrue}^G$  and  $v_{ztrue}^G$  are respectively the position and speed values of the original data of GPS sensor processed by NMEA-0183 protocol and converted to the local coordinate system.  $n_g, n_{g_z}, n_{g_v}$  and  $n_{g_{v_z}}$  are the drift errors of GPS horizontal position, vertical position, horizontal velocity and vertical velocity respectively, which are simplified into Gauss white noise whose variance is  $\sigma_g^2, \sigma_{g_z}^2, \sigma_{g_v}^2$  and  $\sigma_{g_{v_z}}^2$ .

### 3. Federated filter for integrated navigation system

The self-designed solar vector measuring device is used to measure the solar vector, and it is combined with magnetometer, inertial device and GPS as the information source of integrated navigation federal filter.

The attitude quaternion  $\mathbf{q}$ , position  $\mathbf{P}$ , speed  $\mathbf{v}$ , and acceleration deviation  $\mathbf{b}_a$  of UAV is selected under navigation constitute the state vector  $\mathbf{x}$  of UAV.

$$\mathbf{x} = \begin{bmatrix} \mathbf{q}^T & \mathbf{p}^T & \mathbf{v}^T & \mathbf{b}_a^T \end{bmatrix}_{13 \times 1}^T \quad (11)$$

Since the state variables of each sub-filter in the federated filter designed in this paper are the same as those of the main filter, the time updating process of the state variables and the estimated mean square error matrix is only carried out in the main filter, reducing the computational burden of the algorithm [9]. Using the technique of variance upper bound, the updated mean square error matrix in the main filter is assigned to the sub-filter according to the information allocation strategy

$$\mathbf{P}_{i,k/k-1} = \beta_i^{-1} \mathbf{P}_{f,k/k-1} \quad (12)$$

where  $\mathbf{P}_f$  and  $\mathbf{P}_i$  indicate the estimated mean square error matrix in the main filter and sub-filter respectively,  $\beta_i$  is the information allocation factor. The algorithm of information dynamic allocation based on the trace of covariance matrix is used in the

calculation of

$$\beta_{i,k} = \frac{\text{trace}(\mathbf{P}_{i,k-1})}{\sum_{i=1}^N \text{trace}(\mathbf{P}_{i,k-1})}, \quad i = 1, 2, \dots \quad (13)$$

Then the updated prediction information  $\hat{\mathbf{x}}_{f,k,k-1}$  of the main filter state time is transmitted to the sub-filter state prediction information  $\hat{\mathbf{x}}_{i,k/k-1}$

$$\hat{\mathbf{x}}_{i,k/k-1} = \hat{\mathbf{x}}_{f,k,k-1} \quad (14)$$

The federated filter structure of fault tolerant integrated navigation system is shown in figure 3. SINS carries out time update of  $\mathbf{q}, \mathbf{P}$ , and  $\mathbf{v}$  through the main filter, and sends the predictive information to the sub-filter respectively. Sub-filter 1 USES the measured solar vector and the position and velocity information obtained by GPS to measure and update the state quantity prediction information passed in by the main filter, and then passes the measurement update results to the main filter for fusion update. The two sub-filters use different sensors to update the attitude quaternions in the state variables. Even when one of the sub-filters fails, the main filter can output the attitude, position and velocity information accurately.

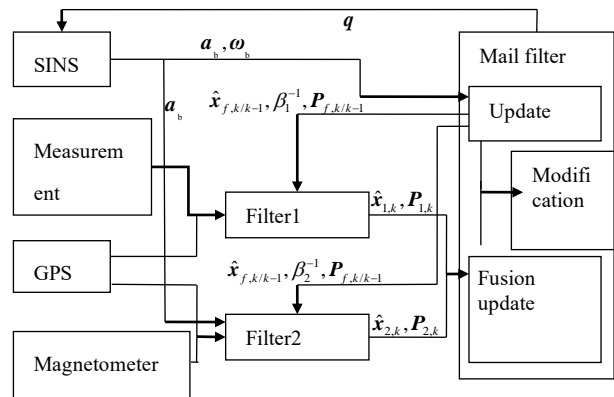


Fig.3 The federal filter structure of fault-tolerant integrated navigation system

#### 3.1 Main filter time update and information fusion

At the initial time of filter operation, all the state vectors except and are set to 0. At this point, as a result of unmanned aerial vehicle (UAV) in a stationary state, the accelerometer and magnetic field to measure the attitude quaternion is relatively accurate, so will subsystem 2 measurement quaternion as state variables in the initial value of quaternion to ensure unmanned aerial vehicle (UAV), whether in a horizontal position, filter can accurately estimate the unmanned aerial vehicle (UAV) initial stance. Choose the differential equation of quaternion as the time update of quaternion in state quantity

$$\dot{\mathbf{q}} = \frac{1}{2} \boldsymbol{\Omega} \mathbf{q} \quad (15)$$

where

$$\boldsymbol{\Omega} = \begin{bmatrix} 0 & -w_b^x & -w_b^y & -w_b^z \\ w_b^x & 0 & w_b^z & -w_b^y \\ w_b^y & -w_b^z & 0 & w_b^x \\ w_b^z & w_b^y & -w_b^x & 0 \end{bmatrix} \quad (16)$$

Acceleration of UAV in navigation system

$$\mathbf{a}_n = \mathbf{C}_b^n \mathbf{a}_b - \mathbf{g} \quad (17)$$

where  $\mathbf{C}_b^n$  is the transformation matrix from the aircraft system to the navigation system, and  $\mathbf{g}$  is the gravity vector.  $\mathbf{a}_n$  as the input of system state time update to get the time update of velocity state quantity

$$\dot{\mathbf{v}} = -\mathbf{C}_b^n \mathbf{b}_a + \mathbf{a}_n \quad (18)$$

Substitute equation (9) and equation (17) into the above equation and arrange

$$\dot{\mathbf{v}} = \mathbf{C}_b^n (\mathbf{a}_b^{true} + \mathbf{n}_a) - \mathbf{g} \quad (19)$$

Similarly, the time update of the position state quantity

$$\dot{\mathbf{p}} = \mathbf{v} \quad (20)$$

The flight state model of the main filter is

$$\dot{\mathbf{x}}_f = \mathbf{A}\mathbf{x}_f + \mathbf{B}\mathbf{a}_n \quad (21)$$

where

$$\mathbf{A} = \begin{bmatrix} \frac{1}{2}\boldsymbol{\Omega} & \mathbf{0}_{4*3} & \mathbf{0}_{4*3} & \mathbf{0}_{4*3} \\ \mathbf{0}_{3*4} & \mathbf{0}_{3*3} & \mathbf{I}_{3*3} & \mathbf{0}_{3*3} \\ \mathbf{0}_{3*4} & \mathbf{0}_{3*3} & \mathbf{0}_{3*3} & -\mathbf{C}_b^n \\ \mathbf{0}_{3*4} & \mathbf{0}_{3*3} & \mathbf{0}_{3*3} & \mathbf{0}_{3*3} \end{bmatrix}_{13*13} \quad (22)$$

$$\mathbf{B} = \begin{bmatrix} \mathbf{0}_{7*3} \\ \mathbf{I}_{3*3} \\ \mathbf{0}_{3*3} \end{bmatrix}_{13*3} \quad (23)$$

The fourth order Runge-Kutta method is used to discretize equation (21)

$$\begin{cases} \mathbf{S}_1 = \mathbf{A}\hat{\mathbf{x}}_{f,k-1} + \mathbf{B}\mathbf{a}_n \\ \mathbf{S}_2 = \mathbf{A}(\hat{\mathbf{x}}_{f,k-1} + \mathbf{S}_1 T_h / 2) + \mathbf{B}\mathbf{a}_n \\ \mathbf{S}_3 = \mathbf{A}(\hat{\mathbf{x}}_{f,k-1} + \mathbf{S}_2 T_h / 2) + \mathbf{B}\mathbf{a}_n \\ \mathbf{S}_4 = \mathbf{A}(\hat{\mathbf{x}}_{f,k-1} + \mathbf{S}_3 T_h) + \mathbf{B}\mathbf{a}_n \end{cases} \quad (24)$$

where  $T_h$  is the sampling period,  $\hat{\mathbf{x}}_{f,k-1}$  is the result of the fusion of the optimal estimation value of the sub-filter state by the main filter at time  $k-1$ , then

$$\hat{\mathbf{x}}_{f,k} = \mathbf{P}_{f,k} [\mathbf{P}_{1,k}^{-1} \hat{\mathbf{x}}_{1,k} + \mathbf{P}_{2,k}^{-1} \hat{\mathbf{x}}_{2,k}] \quad (25)$$

where  $\mathbf{P}_{f,k}$  is obtained by fusion  $\mathbf{P}_{i,k}^{-1}$

$$\mathbf{P}_{f,k} = [\mathbf{P}_{1,k}^{-1} + \mathbf{P}_{2,k}^{-1}]^{-1} \quad (26)$$

From equation (24), we can get the inside differentiation of the predicted value

$$d\mathbf{x}_f = (\mathbf{S}_1 + 2\mathbf{S}_2 + 2\mathbf{S}_3 + \mathbf{S}_4) T_h / 6 \quad (27)$$

$\mathbf{x}_f$  is the one-step prediction obtained by the main filter

$$\hat{\mathbf{x}}_{f,k/k-1} = \hat{\mathbf{x}}_{f,k-1} + d\mathbf{x}_f \quad (28)$$

The one-step prediction of the mean square error differential  $\mathbf{x}_f$  is calculated

$$d\mathbf{P}_f = (\mathbf{A}\mathbf{P}_{f,k-1} + \mathbf{P}_{f,k-1}\mathbf{A}^T + \mathbf{B}\mathbf{R}_u\mathbf{B}^T + \mathbf{Q})T_h \quad (29)$$

where  $\mathbf{R}_u$  is the variance matrix of system input noise, and  $\mathbf{Q}$  is the variance matrix of system process noise. One-step prediction of the mean square error matrix of the winner filter

$$\mathbf{P}_{f,k/k-1} = \mathbf{P}_{f,k-1} + d\mathbf{P}_f \quad (30)$$

### 3.2 Sub-filter 1 measurement update

Assuming that the unitary solar vector  $\mathbf{s}_n$  is measured under the navigation system and  $\mathbf{s}_n$  is considered to be constant in a short time, the projection  $\mathbf{s}_n$  is

$$\mathbf{s}_b = \mathbf{C}_n^b \mathbf{s}_n = \mathbf{h}(q) = [h_{11} \quad h_{21} \quad h_{31}]^T \quad (31)$$

where  $\mathbf{C}_n^b$  is the rotation matrix of navigation system, and

$$h_{11} = s_n^x (q_0^2 + q_1^2 - q_2^2 - q_3^2) + 2s_n^y (q_1 q_2 + q_0 q_3) + 2s_n^z (q_1 q_3 - q_0 q_2)$$

$$h_{21} = 2s_n^x (q_1 q_2 - q_0 q_3) + s_n^y (q_0^2 - q_1^2 + q_2^2 - q_3^2) + 2s_n^z (q_0 q_1 + q_2 q_3)$$

$$h_{31} = 2s_n^x (q_1 q_3 + q_0 q_2) + 2s_n^y (q_2 q_3 - q_0 q_1) + s_n^z (q_0^2 - q_1^2 - q_2^2 + q_3^2)$$

For each row of  $\mathbf{h}(q)$ , the first-order components of Taylor's expansion are taken to obtain the observation matrix of the sun vector under the machine system.

$$\mathbf{H}_s = \begin{bmatrix} \frac{\partial h_{i1}}{\partial \mathbf{q}^T} \end{bmatrix}_{3*4}, i = 1, 2, 3 \quad (32)$$

Then, the observation equation of solar vector under the machine system

$$\mathbf{s}_{b,k}^o = \mathbf{H}_{s,k} \hat{\mathbf{q}}_{1,k/k-1} \quad (33)$$

$\mathbf{s}_{b,k}^o$  is the observed value of solar vector under machine system. Since the one-step predicted value  $\hat{\mathbf{q}}_{1,k/k-1}$  of quaternion in sub-filter 1 is part of the one-step predicted value  $\hat{\mathbf{x}}_{1,k/k-1}$  of state quantity, then the observation matrix  $\mathbf{H}_{1,k}$  of sub-filter 1

$$\mathbf{H}_{1,k} = \begin{bmatrix} \mathbf{H}_{s,k} & \mathbf{0}_{3*6} & \mathbf{0}_{3*3} \\ \mathbf{0}_{6*4} & \mathbf{I}_{6*6} & \mathbf{0}_{6*3} \end{bmatrix}_{9*13} \quad (34)$$

The measuring vector of sub-filter 1 can be obtained by solar vector measuring device and GPS

$$\mathbf{Z}_{1,k} = [\mathbf{s}_b^{mT} \quad \mathbf{p}^{GT} \quad \mathbf{v}^{GT}]^T \quad (35)$$

For the sub-filter, the measurement update process is

$$\begin{cases} \mathbf{P}_{i,k}^{-1} = \mathbf{P}_{i,k/k-1}^{-1} + \mathbf{H}_{i,k}^T \mathbf{R}_i^{-1} \mathbf{H}_{i,k} \\ \mathbf{P}_{i,k}^{-1} \hat{\mathbf{x}}_{i,k} = \mathbf{P}_{i,k/k-1}^{-1} \hat{\mathbf{x}}_{i,k/k-1} + \mathbf{H}_{i,k}^T \mathbf{R}_i^{-1} \mathbf{Z}_{i,k} \end{cases} i=1,2 \quad (36)$$

where  $\mathbf{R}_i$  is the variance matrix of measurement noise.

### 3.3 Sub-filter 2 measurement update

The projection of a unitized gravity vector in body coordinates

$$\mathbf{k} = \frac{\mathbf{a}_b - \mathbf{C}_n^b \dot{\mathbf{v}}^G}{\|\mathbf{a}_b - \mathbf{C}_n^b \dot{\mathbf{v}}^G\|} \quad (37)$$

Ignoring the local magnetic deviation angle, the geomagnetic vector is projected onto the X-axis of the navigation system, and the projection under the machine system is calculated

$$\mathbf{i} = \frac{\mathbf{m}_b - \mathbf{k}(\mathbf{m}_b \mathbf{k})}{\|\mathbf{m}_b - \mathbf{k}(\mathbf{m}_b \mathbf{k})\|} \quad (38)$$

Direction cosine matrix of UAV attitude can be obtained

$$\mathbf{R}_{dcm} = [\mathbf{i} \quad \mathbf{j} \quad \mathbf{k}]^T \quad (39)$$

where  $\mathbf{j}$  is the unit vector perpendicular to  $\mathbf{k}$  and  $\mathbf{i}$ , and conforms to the right hand rule.

The optimal orthogonalization method is used to extract the attitude quaternion from the direction cosine matrix  $\mathbf{q}_m$

$$\begin{cases} |q_{m0}| = \frac{1}{2} \sqrt{1 + \mathbf{R}_{dcm}(1,1) + \mathbf{R}_{dcm}(2,2) + \mathbf{R}_{dcm}(3,3)} \\ |q_{m1}| = \frac{1}{2} \sqrt{1 + \mathbf{R}_{dcm}(1,1) - \mathbf{R}_{dcm}(2,2) - \mathbf{R}_{dcm}(3,3)} \\ |q_{m2}| = \frac{1}{2} \sqrt{1 - \mathbf{R}_{dcm}(1,1) + \mathbf{R}_{dcm}(2,2) - \mathbf{R}_{dcm}(3,3)} \\ |q_{m3}| = \frac{1}{2} \sqrt{1 - \mathbf{R}_{dcm}(1,1) - \mathbf{R}_{dcm}(2,2) + \mathbf{R}_{dcm}(3,3)} \end{cases} \quad (40)$$

$\text{sign}(q_{m0})$  is optional, and  $\mathbf{q}_m$  is determined by the following formula

$$\begin{cases} \text{sign}(q_{m1}) = \text{sign}(q_{m0}) \text{sign}(\mathbf{R}_{dcm}(3,2) - \mathbf{R}_{dcm}(2,3)) \\ \text{sign}(q_{m2}) = \text{sign}(q_{m0}) \text{sign}(\mathbf{R}_{dcm}(1,3) - \mathbf{R}_{dcm}(3,1)) \\ \text{sign}(q_{m3}) = \text{sign}(q_{m0}) \text{sign}(\mathbf{R}_{dcm}(2,1) - \mathbf{R}_{dcm}(1,2)) \end{cases} \quad (41)$$

Then the measurement vector of sub-filter 2 is as follows

$$\mathbf{Z}_{2,k} = [\mathbf{q}_m^T \quad \mathbf{p}^{GT} \quad \mathbf{v}^{GT}]^T \quad (42)$$

Since the variables in are included in the state variables, the observation matrix of sub-filter 2 is

$$\mathbf{H}_{2,k} = [\mathbf{I}_{10 \times 10} \quad \mathbf{0}_{10 \times 3}]_{10 \times 13} \quad (43)$$

Then, the measurement update of sub-filter 2 is obtained from equation (36).

## 4. Simulation results and analysis

MATLAB simulation was carried out for the algorithm designed in this paper, with a given simulation step size of 0.01s and simulation time of 30s. Let  $\sigma_g^2 = \sigma_{gv}^2 = 25$ ,  $\sigma_s^2 = 10^{-4}$ ,

$\sigma_\omega^2 = 4 \times 10^{-2}$ ,  $\sigma_a^2 = 2.1 \times 10^{-3}$ ,  $\sigma_m^2 = 2.1 \times 10^{-3}$ . At the same time, the ideal motion model of UAV is accelerated from horizontal static state at a constant height, and the attitude Angle is sinusoidal. The axial position, velocity and pitch Angle curves of the ideal motion model under the navigation system are as follows

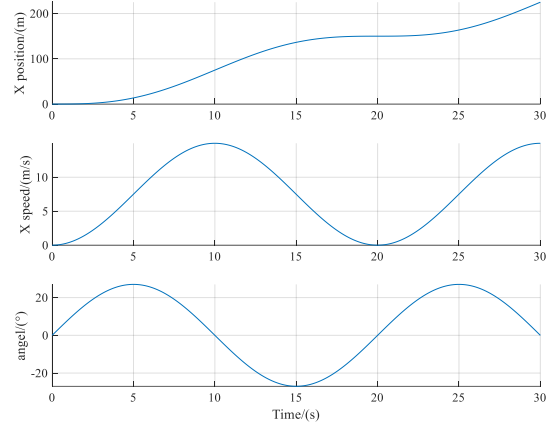


Fig.4 UAV motion curve

Using the federated filter to estimate the navigation status of the UAV, the simulation figure of the difference between the optimal estimation value of the federated filter and the given position and speed of the model is as follows.

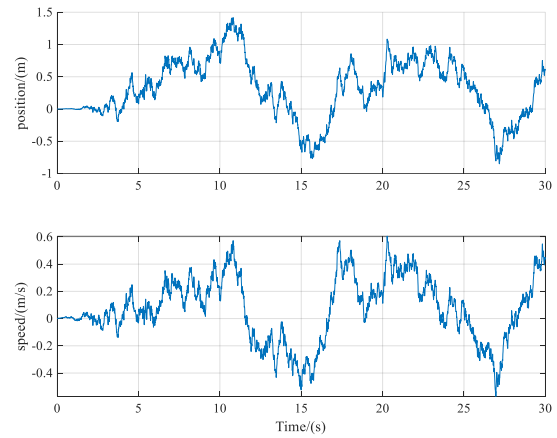


Fig.5 The error curve of position and velocity

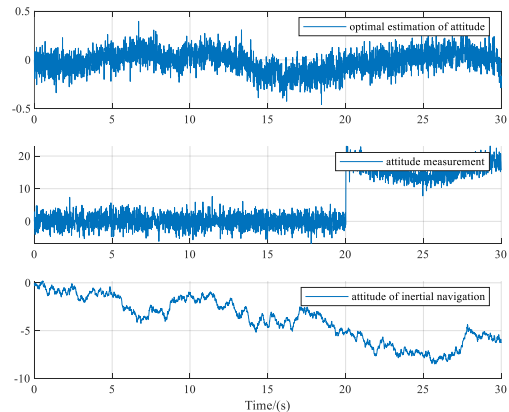


Fig.6 The comparison of pitch angle error curve of federal filter

According to the Gaussian noise added to the accelerometer and GPS, it can be seen that the position and velocity estimated by the federated filter are more accurate.

The pitching Angle of UAV was taken as the simulation attitude Angle, and the simulation comparison between the optimal estimation value of federated filter, the measurement value of sub-filter 2 and the output value of SINS and the difference value of the given pitching Angle of the model was obtained as shown in figure 6.

It can be seen that the federated filter basically reduces the pitch Angle error to less than 0.2 degrees.

Suppose that the system simulation to 20s, the sub-filter 2 magnetometer is interfered and the output magnetic vector is constant.

When the sub-filter fails due to interference, the simulation comparison of pitch Angle error is shown in figure 7.

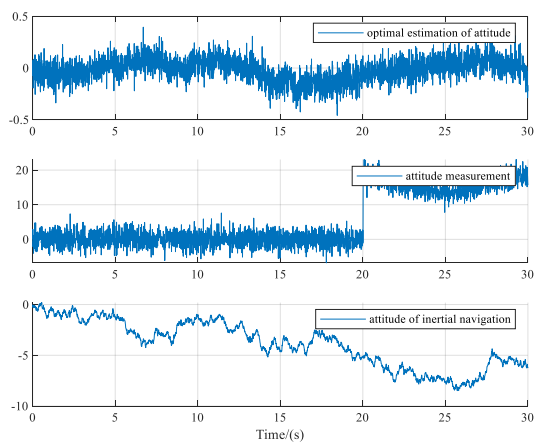


**Fig.7** The comparison of pitch angle error curve when sub-filter fault of federal filter

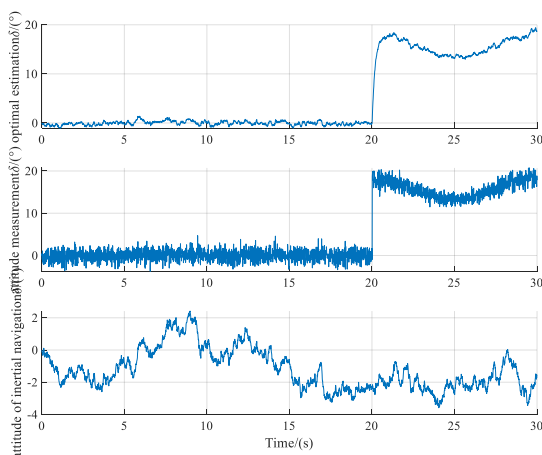


**Fig.8** The comparison of pitch angle error curve when magnetometer fault of Kalman filter

It can be seen that in the second 20s of simulation, due to the fault that the output of the magnetometer is constant, the pitching Angle error measured by sub-filter 2 shows a jump change, while the pitching Angle estimation accuracy of the federated filter does not change significantly.

The results show that the proposed algorithm is fault tolerant to some extent.

In the same simulation condition, the combination navigation of

kalman filter is simulated by subfilter 2 and SINS.

In the second 20s, if the magnetometer appears the same fault as in the simulation in the figure, the simulation result of pitch Angle error is shown in figure 8.

It can be seen from the figure that the pitching Angle error estimated by the kalman filter shows a jump change at the 20s.

Simulation shows that kalman filter integrated navigation can not deal with the fault of magnetometer.

## 5. Summary

The magnetometer is vulnerable to electromagnetic interference in the environment, which makes the attitude estimation of navigation system inaccurate. For this reason, designs a solar vector measuring device, which is used as one of the measuring sensors of the federal filter neutron filter, and proposes the Kalman united filter integrated navigation algorithm. The simulation results show that the federated filter combined navigation algorithm not only improves the accuracy, but also has fault tolerance to sensor faults, which enhances the reliability of the navigation system.

## Acknowledgements

Bhaganagar would like to acknowledge financial support provided by Maine Space Grant Consortium and Hsu would like to acknowledge National Science Foundation (OCE-0644497; CBET-0426811).

## References

- [1] Gao B, Hu G, Gao S, et al. Multi-sensor Optimal Data Fusion for INS/GNSS/CNS Integration Based on Unscented Kalman Filter[J]. International Journal of Control Automation & Systems, 2018, 16(1):129-140.
- [2] Pan J L, Zhi X, Wang L N, et al. A Simplified UKF Algorithm for SINS/GPS/CNS Integrated Navigation System in Launch Inertial Coordinate System[J]. Acta Armamentarii, 2015, 36(3):484-491.
- [3] Yang S, Yang G, Zhu Z, et al. Stellar Refraction-Based SINS/CNS Integrated Navigation System for Aerospace Vehicles[J]. Journal of Aerospace Engineering, 2016, 29(2):04015051.
- [4] Won D H, Lee E, Heo M, et al. Selective Integration of GNSS, Vision Sensor, and INS Using Weighted DOP Under GNSS-Challenged Environments[J]. IEEE Transactions on Instrumentation & Measurement, 2014, 63(9):2288-2298.
- [5] Fresk E, Nikolakopoulos G, Gustafsson T. A Generalized Reduced-Complexity Inertial Navigation System for Unmanned Aerial Vehicles[J]. IEEE Transactions on Control Systems Technology, 2016, 25(1):192-207.
- [6] Sebesta K D, Boizot N. A Real-Time Adaptive High-Gain EKF, Applied to a Quadcopter Inertial Navigation System[J]. IEEE Transactions on Industrial Electronics, 2014, 61(1):495-503.
- [7] Liang Y, Jia Y. A nonlinear quaternion-based fault-tolerant SINS/GNSS integrated navigation method for autonomous UAVs[J]. Aerospace Science & Technology, 2015, 40:191-199.
- [8] LI, S. & CHEN, L. 2018. Research on Object Detection Algorithm Based on Deep Learning. International Journal of Applied Mathematics in Control Engineering, 1, 17-25.
- [9] LIN, S., WU, Z., QI, Y. & HAN, Z. 2018. An Intrusion Detection Method of Internet of Things Based on Agent. International Journal of Applied Mathematics in Control Engineering, 1, 39-46
- [10] SHAO, M., LV, F., DU, W. & SONG, X. 2018. KNN Transition Period Fault Detection Based on Random Projection. International Journal of Applied Mathematics in Control Engineering, 1, 62-69.



**Hongmei Zhang** received the PhD degree in Control Theory & Control Engineering from Tianjin University, China, in 2012. She worked at Shenyang Aerospace University as an associate professor. Her research interests include guidance, navigation and control, optimal control and nonlinear control with their applications.



**Huaqing Zhang** is currently pursuing her M.S. study at Shenyang Aerospace University. He obtained her BS degree from Hebei University of Science and Technology, China in 2017. His research interests include guidance, navigation and control, optimal control and nonlinear control with their applications.